PROCEEDINGS OF SCIENCE

The pNAB experiment and the quest for ever better neutron beam polarization

S. Baeßler,[a,b,*] R. Alarcon,[c] L. Barrón Palos,[d] L. J. Broussard,[b] J. H. Choi,[e] T. Chupp,[f] C. B. Crawford,[g] G. Dodson,[h] N. Fomin,[i] J. Fry,[j] F. Gonzalez,[b] J. Hamblen,[k] L. Hayen,[l] A. Jezghani,[m] M. Makela,[n] R. Mammei,[o] A. Mendelsohn,[p] P. E. Mueller,[b] S. Penttilä,[b] J. A. Pioquinto,[a] B. Plaster,[g] D. Počanić,[a] A. Saunders,[b] W. Schreyer[b] and A. R. Young[e] (the pNAB collaboration)

[a] *Department of Physics, University of Virginia, Charlottesville, VA 22904–4714, USA*

[b] *Physics Division, Oak Ridge National Laboratory, [†] Oak Ridge, TN 37831, USA*

[c] *Department of Physics, Arizona State University, Tempe, AZ 85287–1504, USA*

[d] *Instituto de Física, Universidad Nacional Autónoma de México, Mexico*

[e] *Department of Physics, North Carolina State University, Raleigh, NC 27695-8202, USA*

[f] *University of Michigan, Ann Arbor, MI 48109, USA*

[g] *Department of Physics and Astronomy, University of Kentucky, Lexington, KY 40506, USA*

[h] *Massachusetts Institute of Technology, Cambridge, MA 02139, USA*

[i] *Department of Physics and Astronomy, University of Tennessee, Knoxville, TN 37996, USA*

[j] *Department of Physics, Geosciences, and Astronomy, Eastern Kentucky University, Richmond, KY 40475, USA*

[k] *Department of Chemistry and Physics, Univ. of Tennessee-Chattanooga, Chattanooga, TN 37403, USA*

[l] *Laboratoire de Physique Corpusculaire, Caen, France*

[m] *Partnership for an Advanced Computing Environment, Georgia Institute of Technology, Atlanta, GA 30332, USA*

[*] Speaker

[†] This manuscript has been authored in part by UT-Battelle, LLC, under contract DE-AC05-00OR22725 with the US Department of Energy (DOE). The publisher acknowledges the US government license to provide public access under the DOE Public Access Plan (http://energy.gov/downloads/doe-public-access-plan).

© Copyright owned by the author(s) under the terms of the Creative Commons Attribution-NonCommercial-NoDerivatives 4.0 International License (CC BY-NC-ND 4.0).

[n] *Los Alamos National Laboratory,*
Los Alamos, NM 87545, USA
[o] *Department of Physics, University of Winnipeg,*
Winnipeg, Manitoba R3B2E9, Canada
[p] *Department of Physics and Astronomy, University of Manitoba,*
Winnipeg, Manitoba, R3T 2N2, Canada
E-mail: baessler@virginia.edu

The Nab and pNAB collaborations are conducting a program of studies of free neutron beta decay, with the primary goal of testing the unitarity of the Cabbibo-Kobayashi-Maskawa matrix that describes quark mixing due to the weak interaction. For this purpose, a large, novel electromagnetic spectrometer, the Nab spectrometer, has been designed, built, and placed in use to determine the correlation coefficients in unpolarized neutron beta decay: a, the neutrino–electron correlation coefficient; and b, the Fierz term. The subject of this paper is pNAB, the second phase of the program, that will deploy the same spectrometer with a polarized neutron beam to determine A, the beta asymmetry; and B, the neutrino asymmetry coefficients. A focus of this paper will be on the strategies to provide a high and precisely known neutron beam polarization.

**** 2024 Workshop on Polarized Sources, Targets, and Polarimetry ****
**** 22-27 September, 2024 ****
**** Jefferson Lab, Newport News, VA, USA ****

1. Introduction

There is an opportunity for free neutron beta decay to offer a competitive test of unitarity of the Cabibbo-Kobayashi-Maskawa (CKM) matrix, one of the most sensitive tests of our understanding of the electroweak interaction of quarks. If the Standard Model of Elementary Particle Physics (SM) with three generations completely describes flavor-changing weak interactions, unitarity provides constraints on combinations of the CKM matrix elements. However, providing for beyond-Standard Model physics, the matrix elements of the first row, V_{ud}, V_{us} and V_{ub}, just obey

$$|V_{ud}|^2 + |V_{us}|^2 + |V_{ub}|^2 = 1 - \Delta \quad . \tag{1}$$

The SM requires CKM unitarity, that is $\Delta = 0$. To test that prediction, one determines V_{ud} from nuclear, neutron, or pion beta decay and V_{us} from certain kaon decays. The contribution of V_{ub} is too small to register at the present level of precision. Current experiments indicate $\Delta \sim 10^{-3}$. Refs. [1–4] use an effective field theory (EFT) approach to show that this test of the CKM unitarity is sensitive to physics with a reach comparable to that of the CERN Large Hadron Collider, motivating intensive development of future low energy experiments and also new analysis tools that incorporate both high-energy and low-energy constraints.

The most precise determination of V_{ud} is currently obtained from the analysis of superallowed Fermi (SAF) beta decays. The $\overline{\mathcal{F}t}$ values, the product of "phase space factor", "(partial) half-life", and "nuclear structure and radiative corrections," for multiple nuclides undergoing SAF decays, are averaged and used to determine V_{ud} through

$$|V_{ud}|^2 = \frac{2984.43\ \mathrm{s}}{\overline{\mathcal{F}t}\left(1 + \Delta_R^V\right)} \quad . \tag{2}$$

Since 2018, the inner radiative correction Δ_R^V has been reevaluated, causing a substantial shift and a reduction in its dominant uncertainty, the contribution of the γW box diagram [5–9]. A recent lattice calculation [10] gives a similar value for the inner radiative correction. The analysis of SAF decays in Ref. [11] has recently been updated significantly. Besides the revised inner radiative correction Δ_R^V, it also uses revised nuclear structure-dependent radiative corrections (commonly called δ_{NS} - see also newer work in [12]) that take into account a similarly revised computation of the γW box diagram, now coupling to the whole nucleus [14]. The Particle Data Group (PDG) [13] recognizes the new input and recommends $V_{ud} = 0.97367(11)_{\mathrm{exp.,nucl.}}(13)_{RC}(27)_{NS}$ from SAF decays.

With neutron beta decay, it will be possible to improve the precision of the CKM unitarity test with Eq. (1). The extraction of V_{ud} from neutron and pion beta decay is not affected by nuclear corrections, and the determination of V_{ud} from neutron beta decay benefits from the work on the inner radiative correction similar to SAF decays. The quintuple differential decay rate $d^5\Gamma$ in neutron beta decay at leading order [15] — assuming T-invariance and no detection of spins of the final state particles — has the form

$$d^5\Gamma \propto \rho(E_e) G_F^2 {V_{ud}}^2 \left(1 + a\frac{\vec{p}_e \cdot \vec{p}_\nu}{E_e E_\nu} + b\frac{m_e}{E_e} + \vec{\sigma}_n \cdot \left[A\frac{\vec{p}_e}{E_e} + B\frac{\vec{p}_\nu}{E_\nu}\right]\right) d\Omega_e d\Omega_\nu dE_e \quad . \tag{3}$$

The quantities E_e, E_ν, $\vec{p}_e$, $\vec{p}_\nu$, Ω_e, and Ω_ν are (relativistic) energies, momenta, and solid angles of the electron and neutrino, respectively. The factor G_F is the Fermi constant, $\rho(E_e)$ is a phase

space factor, and $\vec{\sigma}_n$ denotes the neutron spin. At tree-level and upon neglecting terms proportional to the small proton recoil, the interaction is pure $V - A$ (**V**ector minus **A**xial Vector), for which the Fierz interference term b [16] vanishes. The coefficients a and A provide the most sensitive determination of $\lambda = g_A/g_V$, the ratio of the Axial Vector and Vector coupling constants, through

$$a = \frac{1-\lambda^2}{1+3\lambda^2}\,; \quad A = -2\frac{\lambda^2+\lambda}{1+3\lambda^2}\,. \tag{4}$$

The PDG average of existing experimental results leads to $\lambda = -1.2754(13)$ with errors of individual experiments increased by a scale factor of $S = 2.7$. Most of the data used is from measurements of the beta asymmetry A; however, this value is inconsistent at 3σ with the one obtained from measurements of the a coefficient [17, 18].

The quantity V_{ud} from neutron beta decay data is then determined by combining the neutron lifetime τ_n and λ [13]:

$$|V_{ud}|^2 = \frac{5024.7\ \mathrm{s}}{\tau_n\,(1+3\lambda^2)\,(1+\Delta_R^V)} \tag{5}$$

The PDG uses this equation with Δ_R^V as determined in [19], the current average $\lambda = -1.2756(13)$, and the current average lifetime $\tau_n = 878.4(5)$ s. It also notes that the uncertainty in λ is too large.

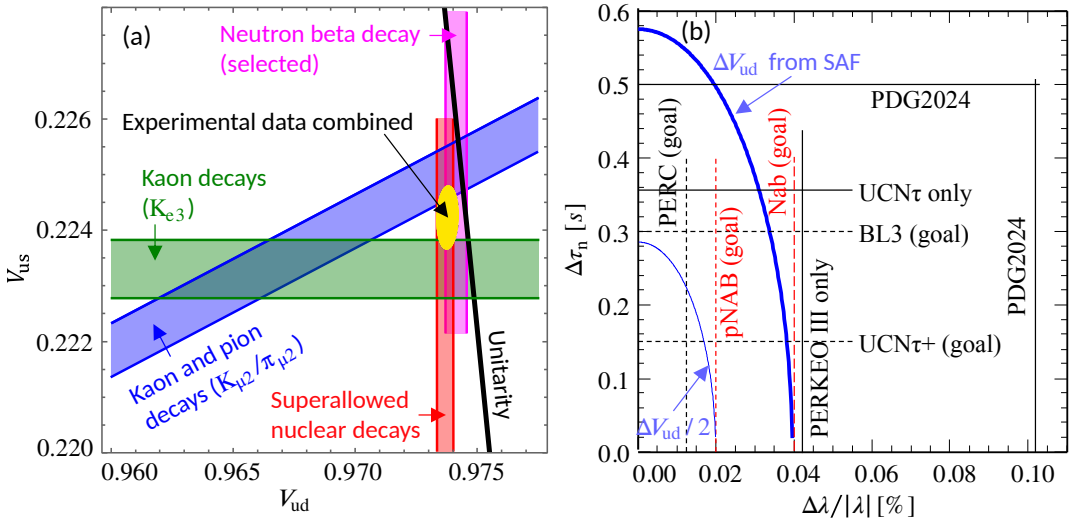

Figure 1: (a) Combined analysis of V_{ud} based on the most precise neutron beta decays and SAF nuclear decays, V_{us}/V_{ud} and V_{us} from kaon and pion decays. If unitarity holds, all 1σ bands have to intersect the black line ($|V_{ud}|^2 + |V_{us}|^2 = 1$) at the same point. The yellow ellipse specifies the 1σ contour of the region with the most likely values for V_{us} and V_{ud} from this analysis; here, unitarity is violated by 2.8σ (analysis and figure from Ref. [19]). (b) Uncertainty ΔV_{ud} from neutron beta decay (Eq. (5)) as a function of uncertainties in the experimental input. Contours of constant values of ΔV_{ud} are ellipses centered on the origin; we show the blue thick contour line for ΔV_{ud} matching that from SAF and the blue thin contour line for half of that value. The outer vertical and horizontal lines show ΔV_{ud} for neutron beta decay, using averages from [13]; their crossing point far from the origin indicates that PDG's average is currently not competitive with SAF. The lines denoted "UCNτ only" and "PERKEO III only" show the selected data set used in Fig. 1(a), which makes neutron beta decay competitive. See also Ref. [20] for a similar plot including nuclear beta decay. Dashed straight lines show the planned impact of new experiments and are discussed in the text.

Figure 1(a) shows a combined analysis of the CKM unitarity test, taken from Ref. [19]. Instead of the usual world average, only the most precise experimental data for λ from a measurement of A in Ref. [21] and τ_n from Ref. [22] from a measurement in a neutron bottle have been included in evaluating the neutron beta decay limit. The V_{ud} values from SAF and neutrons are consistent. The figure also shows the allowed regions from kaon decays. The yellow ellipse combines this experimental input and specifies the 1σ contour of the region with the most likely values for V_{us} and V_{ud}. It misses unitarity, shown by the solid black line, by 2.8σ. Inclusion of recent work to obtain V_{us} from tau decays [3] would increase the deviation.

The goal of the Nab experiment [23–26], currently running at the Fundamental Neutron Physics Beamline (FNPB) of the Spallation Neutron Source (SNS) [27], is to reduce the dominant source of uncertainty in the determination of V_{ud} from Eq. (5) by determining the a coefficient and therefore λ with $\Delta\lambda/|\lambda| = 0.04\%$. This measurement may also shed light on the disagreement between λ as obtained from measuring the a and A coefficients [17, 21, 28]. A natural extension of the Nab experiment will make use of the Nab spectrometer, but with a polarized neutron beam, to perform simultaneous measurements of the β-asymmetry A and neutrino asymmetry B involving polarized neutrons. This experiment, called pNAB, was anticipated in the design of Nab, and thus it will require only minor modification of the existing Nab apparatus. The pNAB experiment will provide a new measurement of λ with a precision goal of $\delta\lambda/|\lambda| = 0.02\%$, using new methods to control sources of systematic uncertainties through coincident detection of electrons and protons and ratios of spin-dependent observables. The Nab and pNAB accuracy goals are illustrated with straight red dashed lines in Fig. 1(b). The new and final results for the neutron lifetime from UCNτ, with accuracy $\Delta\tau_n = 0.3$ s (for the preprint see Ref. [29]), and from J-PARC (for the preprint see Ref. [30]), will make a more substantial impact on the test of the CKM unitarity when they will be accompanied by new results from Nab, pNAB, and PERC [31, 32]. One of them, Nab, is already taking data. The others are proposed or under construction.

Results from pNAB will allow a direct comparison with other beta asymmetry measurements. Should the inconsistencies prevail, their interpretation will benefit from having a determination of λ with Nab and with pNAB, in what is essentially the same spectrometer. There are particular similarities between pNAB and the UCNA+ project, although pNAB remains the only experiment measuring the beta asymmetry A that detects electrons and protons in coincidence. The outcome of this program will not only be a test of the CKM unitarity that avoids uncertainties due to nuclear corrections. The result can also be interpreted as a test of the CVC hypothesis [33] and as a verification of the new radiative correction calculations.

2. Measurement of the beta and the proton asymmetries with the Nab spectrometer

Principles of the pNAB spectrometer design and operation are illustrated in Fig. 2. The neutron beam passes through the polarizer, spin flipper, collimation system, and spectrometer. A tiny fraction of neutrons decay in the fiducial volume. Electrons and protons gyrate around the field lines and eventually hit one of the two silicon detectors [34]. One of the Si detectors is held at -30 kV to allow proton detection. Both Si detectors measure the energy of the decay electrons with a resolution of several keV. Electron energy losses through backscattering of electrons are largely avoided thanks to the magnetic guide field that connects two Si detectors at both ends of

the apparatus. Electrons might bounce, but they are ultimately absorbed in the two detectors, whose signals are added. Only events with a total electron energy above a threshold of 100 keV are considered. Energy loss for detector dead-layer and bremsstrahlung has to be taken into account for electron energy extraction. It is addressed with in-situ calibrations using sets of monoenergetic lines from conversion electron sources and additional measurements in test facilities to fully characterize the energy response of the system. New simulation tools [35] are used in addition to a comprehensive GEANT4 simulation [36] of the Nab spectrometer to address key sources of systematic uncertainty including bremsstrahlung losses.

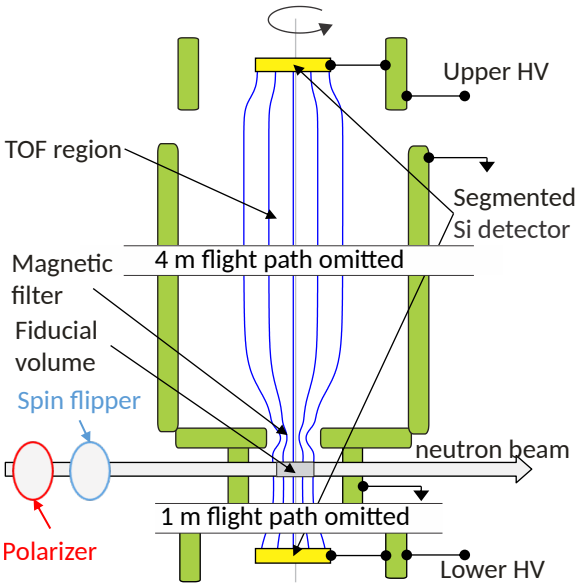

Figure 2: Principles of the design and operation of the pNAB spectrometer. Magnetic field lines (shown in blue) and electrodes (light green boxes) possess cylindrical symmetry around the vertical axis. The spectrometer is currently being used for data taking for Nab. With the addition of a neutron beam polarizer (shown as the red oval) in front of the spin flipper (shown as blue oval), the setup becomes the pNAB spectrometer.

The asymmetry in the count rate of electrons α_e (also called the beta asymmetry) or protons α_p (the proton asymmetry) with respect to the neutron spin can be measured using the Nab spectrometer with minimal modifications; this is the goal of the pNAB experiment. Both count rate asymmetries are of the type

$$d\Gamma \propto \left(1 + \alpha_{e/p} P_n \cos\theta_0\right) \quad , \tag{6}$$

where P_n is the degree of polarization of the neutron beam, and θ_0 the initial angle of electron or proton momentum relative to the neutron beam polarization (i.e., the magnetic field) at the moment of the neutron decay. The quantities α_e or α_p are the observables. They depend on electron and proton energy, although one may average over these dependencies. In all recent beta decay experiments, the electron asymmetry has been measured as a function of electron energy. The result, α_e, is converted into the beta asymmetry A using $\alpha_e = A \cdot p_e/E_e$.

The basic setup for pNAB is close to what is already installed at FNPB for Nab. The pNAB collaboration will add a neutron polarizer before the Nab spectrometer, and modify the spin flipper to make space. Coincidence between electrons and protons from the same neutron decay will be required to suppress background-related uncertainties, a major concern in many of the previous experiments. Our first observable will be α_e. For pNAB, we will use a configuration with an upper detector electrostatic voltage of +1 kV and a lower detector voltage of −30 kV, all voltages relative to the fiducial volume, such that all protons are detected in the lower detector. A positive side effect is the increased rate of coincidence data.

A second measurement is possible with pNAB: The asymmetry α_p can be obtained with the voltage settings as in Nab: $-30\,\mathrm{kV}$ at the upper detector and $-1\,\mathrm{kV}$ at the lower detector. The upper detector serves as the proton detector. Ref. [37] shows how a measurement of the proton asymmetry α_p as a function of the electron energy can be interpreted as a measurement of the neutrino asymmetry B. One experiment of that kind has already been performed, see Ref. [38]. Alternatively, one averages over electron energies and obtains the average proton asymmetry, called C. [1] Furthermore, pNAB also enables the analysis of the ratio of α_e/α_p in the same instrument, with the goal to obtain B/A, as it was done in Ref. [39]. A motivation is that several major systematic effects drop out when this ratio is measured.

In this paper, we are analyzing the measurement of the beta asymmetry A.

2.1 Statistical uncertainty

The pNAB setup enables the detection of essentially all protons in the lower detector and also all electrons with a kinetic energy above an expected threshold of $E_{e,kin,min} = 100$ keV in either detector. Then, the statistical sensitivity of a measurement of the beta asymmetry A in a Standard Model fit ($b = 0$) is $(\Delta A)_{stat} = 4.8/\sqrt{N}$, with N being the number of decays in the fiducial volume. The pNAB goal for the statistical uncertainty, $(\Delta A)_{stat}/|A| = 7 \times 10^{-4}$, requires detection of $N = 5 \times 10^9$ neutron decays. From early beam line characterization [27] and McStas [40] simulations of the collimation system for the Nab spectrometer [41], we expect a neutron capture flux in the fiducial volume of $\Phi_c = 1.3 \times 10^9\ \mathrm{cm^{-2}s^{-1}}$ at a SNS proton beam power of 1.4 MW. [2] With a fiducial volume of $V \sim 240\ \mathrm{cm^3}$ with full solid angle coverage in pNAB, but 20% transmission through the polarizer, we anticipate a decay rate of $320\,\mathrm{s^{-1}}$. With the published schedule for neutron production at SNS [42], and assuming a duty factor of the experiment (not including calibration and other auxiliary measurements) of 75%, the statistical accuracy goal will be reached after about one calendar year.

2.2 Solid angle acceptance for electron detection

In a symmetric spectrometer such as PERKEO III or UCNA, the measurement precision relies on the fact that the accepted solid angle of each detector is a hemisphere. The average cosine of the angle of electron (proton) momentum with the neutron spin in Eq. 6 is $\overline{\cos\theta_0} \sim 1/2$ with a small correction due to the magnetic mirror effect. The asymmetric spectrometer design of Nab eliminates the uncertainty from an unwanted magnetic mirror effect and replaces it with the requirement to determine the solid angle of the upper and lower detectors. The cutoff angle for each detector depends on the magnetic field in the fiducial volume and filter. The measured count rate asymmetries α_e in both detectors can be combined such that the polar angle cutoff for each detector drops out in leading order, as shown in the appendix of Ref. [24], even in the presence of the small magnetic field inhomogeneities in the Nab spectrometer. Therefore, only moderate precision for the magnetic field measurements is needed, and the systematic uncertainty due to the solid angle is

[1] There are different definitions of "proton asymmetry" in the literature; ours follows PDG and also its only measurement [38].

[2] Neutron capture flux Φ_c is defined as an average of the neutron spectral flux $\Phi_\lambda(\lambda_n)$, $\Phi_c = \int \Phi_\lambda(\lambda_n) \cdot \lambda_n/\lambda_{n,0}\, d\lambda_n$, where each neutron is weighted with the efficiency of having a capture or decay event in a given (small) volume relative to a neutron with $\lambda_{n,0} = 1.8$ Å (the average de Broglie wavelength in a thermal neutron beam).

negligible even if taking into account the variation of the magnetic field. One can also neglect the uncertainty from the imperfect knowledge of the neutron beam position, which is responsible for some uncertainty of the average magnetic field in the fiducial volume.

2.3 Neutron beam polarization

A critical point in these measurements will be the precision of the neutron beam polarization measurement. The preferred method to polarize a cold neutron beam, that is, a neutron beam in thermal equilibrium with a cold source and an average de Broglie wavelength of about $\lambda_n = 4$ Å, is to use a supermirror polarizer. A supermirror works as follows: neutrons impinging on a flat surface under a small angle (to the surface) are specularly reflected from that surface due to the neutron optical potential of the surface. That potential is caused by the interaction of the neutron with the nuclei in the surface. The reflectivity of the surface can be enhanced by coating the surface with a multilayer system consisting of thin layers from (usually two) materials with different neutron optical potentials, similar to what is done in light optics. The reflectivity enhancement for a polychromatic neutron beam requires an artful choice of variable layer thicknesses. In a polarizing supermirror, one of these materials in the supermirror is ferromagnetic. In a ferromagnet, the neutron optical potential contribution from the electrons cannot be neglected. The contribution from the electrons changes sign with the spin direction relative to the direction of the magnetization of the ferromagnetic material. The neutron optical potential contribution from the nuclei may be enhanced or reduced with the contribution from the electrons. Thus, the reflectivity of a polarizing supermirror depends on the neutron spin state. With a proper choice of materials, the neutron optical potential of both materials of the supermirror can be made equal, leading to the reflectivity of the supermirror to be small for one spin state, and large for the other.

Much effort in recent decades has been spent to extend the angular range of polarizing (and unpolarizing) supermirrors to larger angles. Fig. 3 shows an example of the reflectivity curve of a modern supermirror that is currently commercially available. The reflectivity for different spin states is given as a function of the angle φ of incoming and outgoing neutron beam to the surface, commonly given as the m value. This is the ratio $m = \varphi/\varphi_{c,Ni}$, where the reference is made to the so-called critical angle of natural nickel $\varphi_{c,Ni}$ ($\varphi_{c,Ni} = \lambda_n \cdot 0.1°/\text{Å}$ with neutron wavelength λ_n). The m value is a function the momentum transfer Q_z of the neutron to the surface in units of the reduced Planck's constant $\hbar$, $Q_z = 4\pi \sin\varphi/\lambda_n$. Additionally, the figure shows the resulting neutron beam polarization, which is the asymmetry in the reflectivity with respect to the neutron spin state. Traditionally, a supermirror polarizer consists of a stack of slightly curved glass substrates coated with polarizing supermirrors. The stack is oriented such that neutrons enter nearly tangential to the surfaces. The slight curvature of the substrates is designed to require each neutron to be reflected at least once from a supermirror surface. Again, reflectivity is high only for one spin state. Neutrons in the other spin state penetrate the multilayer surface and may be absorbed either in a second multilayer coating below the first consisting of materials that have a large neutron capture cross section, or in the glass substrate. For a wide and polychromatic beam of cold neutrons, supermirror polarizers typically achieve polarization efficiencies between 95% and 99%.

Although supermirrors achieve high polarization efficiencies, the efficiency is not uniform over the phase space of the polarized neutron beam. Therefore, it is difficult to determine the average neutron beam polarization with an uncertainty that is much below the order of magnitude of its non-

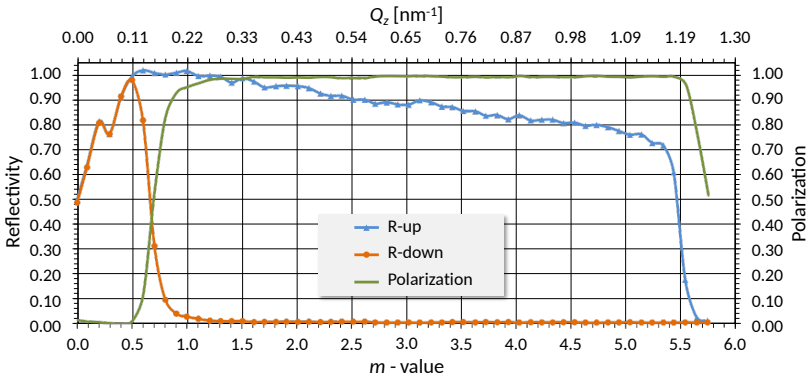

Figure 3: Reflectivity for spin-up ("R-up") and spin-down ("R-down") neutrons, and the resulting neutron beam polarization, of a modern Fe/Si polarizing supermirror [43]. The horizontal axis is a common way to parametrize the angle φ of the incoming and outgoing neutron beam to the surface (see text).

uniformity. In Fig. 3, the polarization is poor for ultra-small angles (Here, $m < 0.7$, corresponding to $\varphi < 0.3°$ for a 4 Å neutron). [3] To minimize the uncertainty in the average polarization of a wide polychromatic beam, a supermirror polarizer should be designed to have a very small non-uniformity [44–47], and that usually makes it also a polarizer with very high polarization efficiency. In fact, the weak point in previous measurements of neutron beta decay correlation coefficients [48, 49] was believed to be the difficulty of a precision measurement of the degree of beam polarization (related to its non-uniformity) provided by polarizing supermirrors. Even after the advent of opaque polarized He-3 cells as analyzers of the average beam polarization [50], the uncertainty in the beam polarization that was provided by a traditional polarizing supermirror device was the largest systematic uncertainty in the current most precise measurement of the beta asymmetry [21].

Reasons for imperfections of the degree of neutron beam polarization are

(a) **grazing incidence:** the reflectivity of the supermirror is large for both spin states under ultra-small incident angles relative to the surface.

(b) **correlated angles:** contrary to naïve expectation, [4] a polarizing device that requires multiple reflections does not necessarily show a strongly improved polarization efficiency. Neutrons that have a very small reflection angle in the first reflection also often have very small reflection angles in subsequent reflections. Typical S-benders have their purpose as they don't bend the polarized beam [51, 52]), but they show only a slightly higher degree of polarization.

(c) **depolarization:** incorrectly magnetized patches often found in thin layers of magnetic materials cause spin flips and limit polarization efficiency [53].

Most supermirror polarizers comprise a stack of long (30 – 50 cm) glass substrates with gaps not much wider than the thickness of the glass substrate in between. The length renders the substrate opaque, and only neutrons that enter through the gaps can be transmitted, with transmission still limited by imperfect reflectivity.

An early attempt for a more substantial improvement of the degree of polarization was the use of two crossed supermirror polarizers [47]; changing directions avoids problem **(b)** of correlations

[3] In experiments where a neutron flux as high as for pNAB is not needed, the neutron beam can be tailored to have a very small wavelength spread and divergence so that it becomes possible to select only favorable parts of the phase space.

[4] A sequence of two polarizing reflections with uncorrelated reflection angles with polarization efficiency P_1 for the first and P_2 for the second has a combined polarization efficiency $P = (P_1+P_2)/(1+P_1P_2) \approx 1-(1-P_1)(1-P_2)/2 \approx 1$, where the approximations are good for $P_1, P_2 \approx 1$ [47]

between the reflection angles in each polarizer and indeed provides a very high degree of polarization, at the cost of even larger transmission losses. The measurement of that degree of polarization with additional supermirrors (the usual method at that time) is again hampered by the fact that the polarization is not uniform over the neutron phase space.

A recent improvement that pNAB plans to use has been developed and tested, and is being operated at Institut Laue-Langevin (ILL) [54]: a modern Solid State Polarizer in V bender geometry (SSPV), building on the idea to have multiple reflections without the drawbacks listed above. The supermirror coating used was optimized to have only a small angular range for unwanted ultra-small angle reflections with mediocre polarization. Neutrons cannot make it through the SSPV with only those reflections, as is shown in the sketch of the setup in Figure 4.

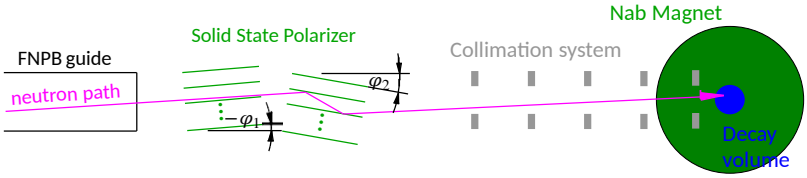

Figure 4: Proposed setup for studies of polarized neutron beta decay with pNAB, top view.

The SSPV consists of two stacks of 180 μm thin sapphire plates oriented at an angle relative to the neutron beam, with modern reflective supermirror coating on the both sides of the substrate, and anti-reflective coating above each of them. In contrast to traditional supermirror polarizers, there are no gaps between the substrate. Neutrons pass through the substrate instead, and one can tolerate the small amount of absorption; the attenuation through a few centimeters of sapphire substrate is less of a limitation than imperfect reflectivity of the supermirror-coated surface of the substrate. Consequentially, neutron transmission is higher than for conventional supermirror polarizers. Most neutrons undergo at least two polarizing reflections (and all at least one), guaranteeing a degree of polarization as large as for crossed supermirror polarizers. Assembly of the SSPV will be done in a clean room to avoid dust that could limit the degree of parallelism of the sapphire plates. The limitation of imperfectly magnetized supermirror material will be suppressed in a much higher than usual magnetic field [55]. Simulations for FNPB [56, 57] predict 99.5% polarization efficiency at 40% transmission just behind the polarizer, [5] which degrades to still 99.5% polarization, but 20% transmission behind the Nab collimation system, in the fiducial volume. Our optimization is necessarily slightly different from what has been done for ILL since the FNPB has a neutron beam with higher divergence [27] than the PF1B beamline at ILL [58]. However, our prediction is similar to the demonstrated performance of the recently built device at ILL: For the ILL device, 99.7% polarization at 33% transmission just behind polarizer were measured [59]. In summary, the SSPV combines high polarization with acceptable transmission. A practical point is that we do not have to move the Nab spectrometer when we switch between polarized and unpolarized neutron beam, as the beam going through the SSPV is not deflected, unlike it would be for the usual supermirror polarizer. The degree of neutron beam polarization will not have the time dependence of a ^{3}He

[5] We define transmission as the ratio of neutron capture flux with and without polarizer. An ideal polarizer would have a transmission of 50%, as we do want to lose one neutron spin state.

polarizer, and the constantly high degree of polarization does not degrade the statistical sensitivity of the experiment.

The systematic uncertainty in pNAB from imperfect neutron beam polarization ΔP_n will be small, due to the fact that the deviation from perfect polarization is small, as demonstrated in all modern beta asymmetry experiments. We plan to measure the neutron beam polarization with opaque ^{3}He cells. We are estimating the uncertainty to be $\Delta P_n \leq 5 \times 10^{-4}$, corresponding to a relative uncertainty in the beta asymmetry of $\Delta A/A \leq 5 \times 10^{-4}$. We consider this a conservative estimate — The ILL group estimates that $\Delta P_n \leq 1 \times 10^{-4}$ is feasible for a beam similar to ours [60]. Corrections have to be applied: the transverse Stern-Gerlach effect increases or decreases the neutron beam vertical extent depending on the neutron spin state when the neutron beam traverses the non-uniform magnetic field at the entrance of the spectrometer. The internal collimation system will preferentially absorb neutrons in a particular spin state. The longitudinal Stern-Gerlach effect causes one neutron spin state to accelerate and the other to decelerate when entering the spectrometer, again causing a slight preference for neutrons with a particular spin to decay in the fiducial volume. Both effects cause a polarization change of the number of decaying neutrons of a few 10^{-4} and are calculable corrections.

In an earlier alternative proposal, it was intended to polarize the neutron beam using a cell containing polarized ^{3}He, relying on the known wavelength-dependence of the neutron beam polarization as a tool to analyze it [61]. This is possible at a pulsed source like the SNS where different wavelengths are associated with different arrival times of the neutrons in the fiducial volume. An advantage of this proposal is that the time dependence of $\alpha_{e/p}$ provides a polarization measurement concurrently with data taking of decay particles. In past experiments, the neutron beam polarization provided by supermirror polarizers was monitored and found to be stable, but for ^{3}He polarizers that is not be the case. With a ^{3}He polarizer, no dedicated polarization measurement runs are needed. Furthermore, no corrections needs to be made for transverse and longitudinal Stern-Gerlach effects, as the polarization is measured inside and not in front of or behind the fiducial volume. A potential issue is that for a reasonable transmission, the neutron beam polarization is lower ($\sim 80\%$) which renders systematic errors hard to detect. The method relies on the assumption that the ^{3}He polarizer is the only device that affects neutron beam polarization, an assumption that has not yet been verified at the required level of precision. Furthermore, at least in past experiments, keeping polarized ^{3}He cells working for long periods (many months) is labor-intensive.

In both methods it is necessary to flip the neutron beam polarization periodically. We are not discussing it here, as an AFP spin flipper for neutrons has been demonstrated to work with very high efficiency (e.g., in Ref. [59], a spin flip efficiency of $f > 0.999$ has been reported). In the alternative proposal, a neutron spin flipper is not even needed, as the AFP flip can be performed on the polarized ^{3}He cell, also with very high efficiency.

2.4 Electron energy calibration

The pNAB experiment plans to use the same detector system as the one used in Nab. The simulated electron energy response of the Nab detector system is shown in Fig. 5(a). The resolution is substantially better than that of plastic scintillator detectors like the ones that were used in previous measurements of the beta asymmetry A. A set of radioactive calibration sources is used to determine the detector response function and to establish the linearity of the relationship between

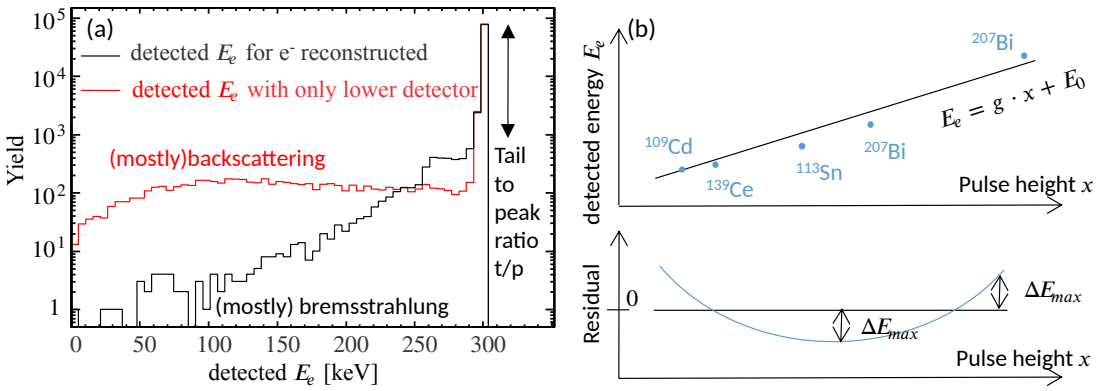

Figure 5: (a) Simulated detector electron energy response for electrons incoming with $E_e = 300\,\text{keV}$. The red curve is for a single detector, and shows a large tail due to electron backscattering. The black curve is the sum of both detectors. The effect of backscattering is suppressed, and the remaining tail is mostly due to Bremsstrahlung. (b) Relationship between energy deposited in a detector and the average pulse height of the output signal. We expect a linear relationship between pulse height x and detected energy E_e, with gain factor g and offset E_0. These simulated data exaggerate possible types of nonlinearity.

deposited energy and ADC channel. The sources are backed by thin foils and are movable within the fiducial volume so as to reach every point in the detector. Possible deviations from perfect linearity of the relationship between pulse height and deposited energy are shown in Fig. 5(b). Table 1 shows the requirements on the detector response to achieve desired measurement uncertainties. The requirements for the measurement of the beta asymmetry A are much less stringent than what the Nab collaboration is trying to achieve in their measurements of the a and b coefficients. Detector design and modeling are described in Refs. [35, 62–64].

Table 1: Requirements on our understanding of the detector response for the planned measurements with Nab and pNAB. The parameters are explained in Fig. 5.

Specification for	$\Delta a = 3 \times 10^{-5}$ (Nab)	$\Delta b = 10^{-3}$ (Nab)	$\Delta A = 3 \times 10^{-5}$ (pNAB)
Gain factor $\Delta g/g$	fit parameter	fit parameter	0.0018
Offset E_0	0.3 keV	0.06 keV	0.2 keV
Nonlinearity $\lvert\Delta E_{\text{max}}\rvert$	1.5 keV	0.06 keV	0.3 keV
Tail to peak ratio $\Delta(t/p)$	0.01%	0.2%	2.4%

3. Summary

The pNAB experiment is proposed to be staged at the FNPB immediately following the completion of measurements with unpolarized neutrons in the Nab experiment, and it will re-use most of the existing Nab apparatus. The most significant hardware addition will be a novel, custom-designed high-efficiency supermirror polarizer.

The first goal of the pNAB experiment is a measurement of the neutron beta asymmetry to substantially better than $\Delta A/A = 10^{-3}$, as indicated in Fig. 1(b). The main systematic uncertainties

in this measurement are related to the determination of the neutron beam polarization and to the detector, and pNAB will have an important synergy with the Nab experiment in that the detector characterizations made for Nab will be more than sufficient for pNAB. Together, the Nab and pNAB measurements will provide a unique study of the CKM matrix unitarity, with very different systematics compared to other existing or planned measurements. CKM unitarity appears to be violated by about $2-3\sigma$ since new, more precise calculations of the inner radiative correction became available, making the proposed pNAB extension to Nab well motivated.

Acknowledgments

We acknowledge the support from the National Science Foundation (in particular from awards 2111363, 2209484, 2209590, 2412782, 2412846), Department of Energy Nuclear Physics (NP) (in particular from awards DE-FG02-03ER41258, DE-FG02-97ER41042, DE-SC0014622 and DE-SC0019309), the University of Virginia, Arizona State University, the Natural Sciences and Engineering Research Council of Canada, and Triangle University Nuclear Laboratory.

References

[1] V. Cirigliano *et al.*, Nucl. Phys. B **830**, 95 (2010)

[2] M. Gonzáles-Alonso *et al.*, Prog. Nucl. Part. Phys. **104**, 165 (2019)

[3] V. Cirigliano *et al.*, J. High En. Phys. **04**, 152 (2022)

[4] V. Cirigliano *et al.*, arXiv: 2311.00021

[5] C.-Y. Seng *et al.*, Phys. Rev. Lett. **121**, 241804 (2018)

[6] C.-Y. Seng *et al.*, Phys. Rev. D **100**, 013001 (2019)

[7] A. Czarnecki *et al.*, Phys. Rev. D **100**, 073008 (2019)

[8] L. Hayen *et al.*, Phys. Rev. D **103**, 113001 (2021)

[9] K. Shiells *et al.*, Phys. Rev. D **104**, 033003 (2021)

[10] P.-X. Ma *et al.*, Phys. Rev. Lett. **132**, 191901 (2024)

[11] J.C. Hardy, I.S. Towner, Phys. Rev. C **102**, 045501 (2020)

[12] V. Cirigliano *et al.*, Phys. Rev. Lett. **133**, 211801 (2024)

[13] S. Navas *et al.* (Particle Data Group), Phys. Rev. D **110**, 030001 (2024)

[14] M. Gorchtein, Phys. Rev. Lett. **123**, 042503 (2019)

[15] J.D. Jackson *et al.*, Phys. Rev. **106**, 517 (1957)

[16] M. Fierz, Z. f. Phys. **104**, 553 (1937)

[17] M. Beck *et al.*, Phys. Rev. Lett. **132**, 102501 (2024)

[18] F.E. Wietfeldt *et al.*, Phys. Rev. C **110**, 015502 (2024)

[19] V. Cirigliano *et al.*, Phys. Lett. B **838**, 137748 (2023)

[20] L. Hayen, Annu. Rev. Nucl. Part. Sci. **74**, 497 (2024)

[21] B. Märkisch *et al.*, Phys. Rev. Lett. **122**, 242501 (2019)

[22] F.M. Gonzalez *et al.*, Phys. Rev. Lett. **127**, 162501 (2021)

[23] D. Počanić *et al.*, Nucl. Inst. Meth. A **611**, 211 (2009)

[24] S. Baeßler *et al.*, J. Phys. G **41**, 114003 (2014)

[25] J. Fry *et al.*, Eur. Phys. J. Web Conf. **219**, 04002 (2019)

[26] S. Baeßler *et al.*, Eur. Phys. J. Web Conf. **303**, 05001 (2024)

[27] N. Fomin *et al.*, Nucl. Instr. Meth. A **773**, 45 (2015)

[28] M.A.P. Brown *et al.*, Phys. Rev. C **97**, 035505 (2018)

[29] R. Musedinovic *et al.*, arXiv: 2409.05560

[30] Y. Fuwa *et al.*, arXiv: 2412.19519

[31] D. Dubbers *et al.*, Nucl. Instr. Meth. A **596**, 238 (2008)

[32] X. Wang *et al.*, Europ. Phys. J. Web Conf. **219**, 04007 (2019)

[33] D. Dubbers, M.G. Schmidt, Rev. Mod. Phys. **83**, 1111 (2011)

[34] L.J. Broussard *et al.*, J. Phys.: Conf. Ser. **876**, 012005 (2017)

[35] L. Hayen *et al.*, Phys. Rev. C **107**, 065503 (2023)

[36] S. Agostinelli *et al.*, Nucl. Instr. Meth. A **506**, 250 (2003)

[37] F. Glück, Nucl. Phys. A **593**, 125 (1995)

[38] M. Schumann *et al.*, Phys. Rev. Lett. **100**, 151801 (2008)

[39] Yu.A. Mostovoi *et al.*, Phys. At. Nucl. **64**, 1955 (2001)

[40] P. Willendrup, K. Lefmann, Journal of Neutron Research **23**, 7 (2021)

[41] E.M. Scott, University of Tennessee Knoxville, Neutronics Report, unpublished (2016)

[42] SNS 5-Year Working Schedule, Available online: https://neutrons.ornl.gov/sites/default/files/Neutron%20Production%20High%20Level%20update%2010_21_24-SNS%20%2C%20HFIR%2011_8.pdf [Accessed Jan 6, 2025].

[43] SwissNeutronics AG, Available online: https://www.swissneutronics.ch/products/neutron-supermirrors/ [Accessed: Nov. 21, 2024].

[44] H. Abele *et al.*, Phys. Lett. B **407**, 212 (1997)

[45] A. Serebrov *et al.*, Journ. Exp. Theo. Phys. **86**, 1074 (1998)

[46] H. Abele *et al.*, Phys. Rev. Lett. **88**, 211801 (2002)

[47] M. Kreuz *et al.*, Nucl. Inst. Meth. A **547**, 583 (2005)

[48] B.G. Yerozolimsky, Nucl. Inst. Meth. A **440**, 491 (2000)

[49] J. Byrne, Nucl. Inst. Meth. A **440**, 781 (2000)

[50] O. Zimmer *et al.*, Phys. Lett. B **455**, 62 (1999)

[51] A. Stunnault *et al.*, Physica B: Condensed Matter **385-386**, 1152 (2006)

[52] Th. Krist *et al*., Nucl. Inst. Meth. A **698**, 94 (2013)

[53] Ch. Klauser *et al*., Nucl. Inst. Meth. A **840**, 181 (2016)

[54] A.K. Petoukhov *et al*., Nucl. Inst. Meth. A **838**, 33 (2016)

[55] A.K. Petoukhov *et al*., Rev. Sci. Instr. **90**, 085112 (2019)

[56] L. Shen, University of Virginia, internal report (2021)

[57] J.A. Pioquinto, University of Virginia, internal report (2024)

[58] H. Abele *et al*., Nucl. Inst. Meth. A **562**, 407 (2006)

[59] A.K. Petoukhov *et al*., Rev. Sci. Instrum. **94**, 023304 (2023)

[60] T. Soldner *et al*., Eur. Phys. J. Web Conf. **219**, 10003 (2019)

[61] S.I. Penttilä, J.D. Bowman, J. Res. Natl. Inst. Stand. Technol. **110**, 309 (2005)

[62] A. Salas Bacci *et al*., Nucl. Instr. Meth. A **735**, 408 (2014)

[63] L.J. Broussard *et al*., Nucl. Instr. Meth. A **849**, 83 (2017)

[64] L.J. Broussard *et al*., Hyp. Int. **240**, 1 (2019)